North to south asymmetries in the water-equivalent hydrogen distribution at high latitudes on Mars

W. C. Feldman,[1] J. L. Bandfield,[2] B. Diez,[3] R. C. Elphic,[4] S. Maurice,[3] and S. M. Nelli[5]

Received 12 October 2007; revised 28 March 2008; accepted 14 May 2008; published 8 August 2008.

[1] Water content and burial depths derived from thermal and epithermal neutron currents measured by the Mars Odyssey Neutron Spectrometer are used to determine north to south asymmetries and intercorrelations at high latitudes on Mars. Our goal is to contrast observed asymmetries with predictions based on current climate conditions and potential regolith thermophysical and chemophysical properties. The average mass fraction of water-equivalent hydrogen within the buried layer is higher on average in the south between 60° and 75° latitude and is strongly anticorrelated with burial depth in both hemispheres. These results argue that the observed water content at high latitudes may require differing north to south thermophysical and/or chemophysical properties of the regolith.

Citation: Feldman, W. C., J. L. Bandfield, B. Diez, R. C. Elphic, S. Maurice, and S. M. Nelli (2008), North to south asymmetries in the water-equivalent hydrogen distribution at high latitudes on Mars, *J. Geophys. Res.*, *113*, E08006, doi:10.1029/2007JE003020.

1. Introduction

[2] A fundamental property of Mars is its asymmetry about its equator. The surface north of the equator is on average about 5 km lower than that south of the equator [*Smith et al.*, 1999]. The residual north polar ice cap is much larger than that near the south pole. In addition, although both caps are composed of thick deposits of water ice, the cap in the north is exposed to the atmosphere, while that in the south is covered by a thin veneer of CO_2 ice [*Kieffer et al.*, 1976; *Kieffer*, 1979]. These conditions work in concert with the present orbital parameters of Mars (which lead to aphelion near the northern summer solstice) to produce an average water-vapor density in the northern hemisphere that is nearly 1.5 times that in the southern hemisphere [*Smith*, 2002].

[3] Yet, a first analysis of leakage neutron currents measured by the Mars Odyssey Neutron Spectrometer (MONS) using a one-dimensional model of surface soils, found the hydrogen abundance, quantified here as water-equivalent hydrogen (WEH) regardless of its actual molecular associations, to be nearly symmetrical about the equator at high latitudes with the south being slightly favored [*Feldman et al.*, 2004]. Both latitude zones between 60° and 75°Contain relative maxima of about 55% to 60% WEH (covering Scandia Colles in the north and just southeast of Hellas Basin in the south) [*Prettyman et al.*, 2004; *Feldman et al.*, 2004], pronounced relative minima of about 10% WEH (centered on Acidalia in the north and just south of Noachis Terra in the south), and broad longitudinal zones that cover the remaining longitudes at these latitudes, which have nearly constant, intermediate abundances of WEH.

[4] We address this apparent discrepancy using a two-dimensional model of the WEH distribution in surface soils [*Diez et al.*, 2008; *Feldman et al.*, 2007]. Our goal is to understand the relationship between the observed WEH content and implied pore volume and mineralogical structure of surface soils, and with inferred past and present climate conditions.

[5] An overview of the data reduction procedure and resultant uncertainties at high latitudes is presented in section 2. Maps of the WEH mass fraction of an assumed semi-infinite lower layer and its apparent burial depth below a relatively desiccated upper layer, are presented in section 3. Quantitative intercomparisons between these distributions as a function of northern and southern latitudes between 60° and 75° are also presented in section 3. A summary of results is given in section 4. Discussions of potential implications of these correlations on the pore volume-fraction structure of surface soils and possible mineralogical composition, and the timing of, and potential delivery mechanisms for near-surface water molecules, are given in section 5.

2. Data Reduction and Systematic Uncertainties

[6] Thermal and epithermal neutron currents measured using the MONS between February 2002 and September 2005 were used for this study. The procedure used to reduce raw counting rates to neutron currents is given by *Maurice*

[1]Planetary Science Institute, Tucson, Arizona, USA.
[2]Department of Earth and Space Sciences, University of Washington, Seattle, Washington, USA.
[3]Centre d'Etude Spatiale des Rayonnements, Toulouse, France.
[4]NASA Ames Research Center, Moffett Field, California, USA.
[5]Atmospheric, Oceanic and Space Sciences, University of Michigan, Ann Arbor, Michigan, USA.

0148-0227/08/2007JE003020

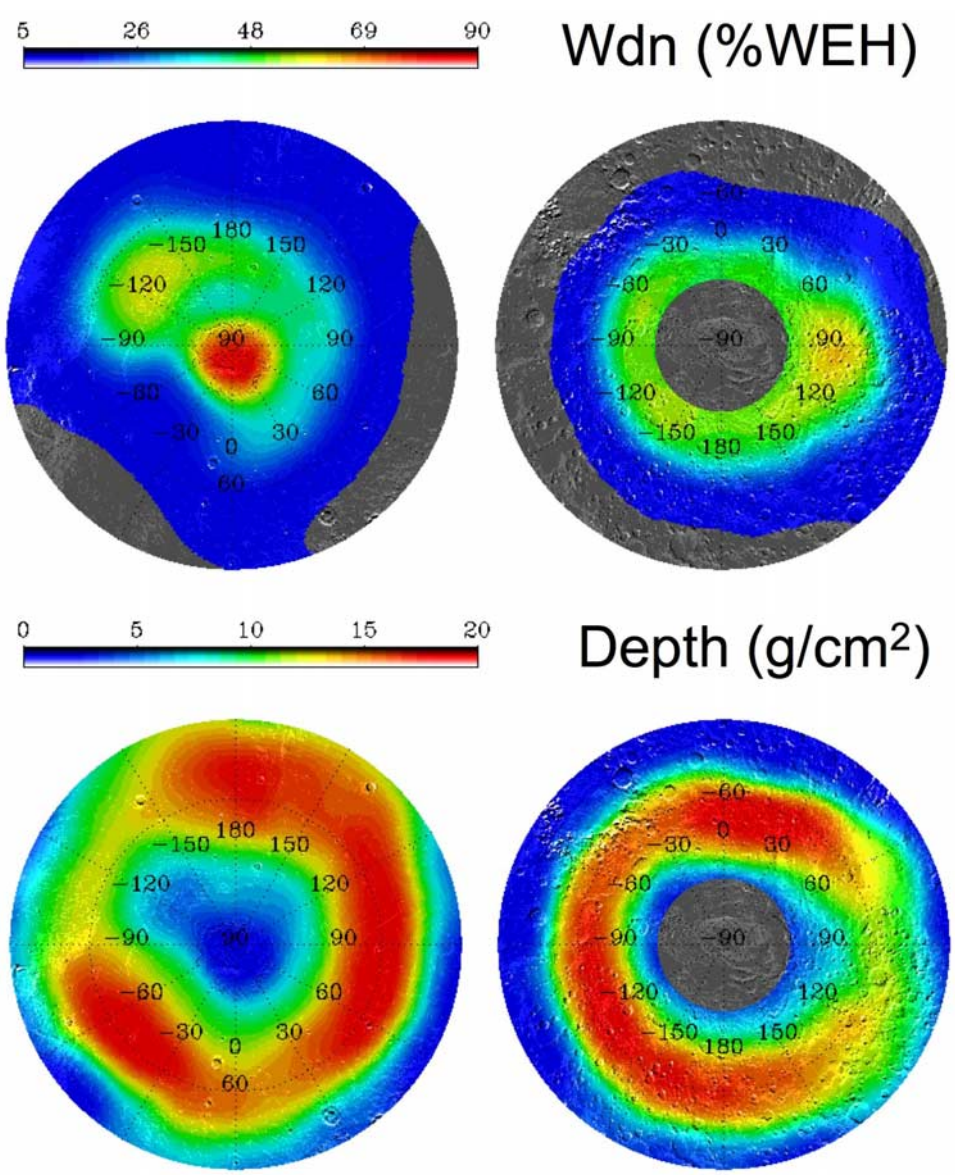

Figure 1. Stereographic projections poleward of ±45° of the water mass fraction of a (top) lower, semi-infinite layer and (bottom) its apparent burial depth (in g/cm^2) beneath a relatively desiccated top layer. WEH, water-equivalent hydrogen.

et al. [2007]. The procedure used in the next stage of reduction to convert these currents to the WEH mass fraction of an assumed semi-infinite lower soil layer, Wdn, and its apparent burial depth, D in g/cm^2, beneath a relatively desiccated upper layer, is given by *Diez et al.* [2008].

[7] The discussion of uncertainties in determinations of Wdn and D given by *Diez et al.* [2008] was global in extent. Three components were identified. The first covered uncertainties in the first stage of reduction [*Maurice et al.*, 2007], which amounted to ±5% for the thermal and epithermal neutron currents, and ±10% for fast neutron currents. We only use the thermal and epithermal neutrons in our present analysis because the uncertainties in determination of fast neutron currents is sufficiently large that they provide little additional information regarding separate determinations of Wdn and D for mapping purposes that differs significantly from that derived from the epithermal neutron currents. Nevertheless, the combination of epithermal and fast neutron currents can be used to show that on average for latitudes higher than 60°, the WEH content of the upper layer, Wup, must be between about 1 wt. % and 5 wt. % [*Feldman et al.*, 2007]. We choose 1 wt. % here because it provides determinations of Wdn and D derived from fast and epithermal neutron currents that are most closely equal to those derived from use of thermal and epithermal neutron currents (however, with relatively large uncertainties).

[8] The remaining two sources of uncertainties stem from our choice of Wup = 1 wt. % WEH in the upper soil layer and the elemental composition (other than hydrogen) of surface soils measured at the Pathfinder landing site [*Wänke et al.*, 2001]. Uncertainties stemming from our choice of 1 wt % were evaluated by determining the sensitivity of derived values of Wdn and D to Wup using data measured

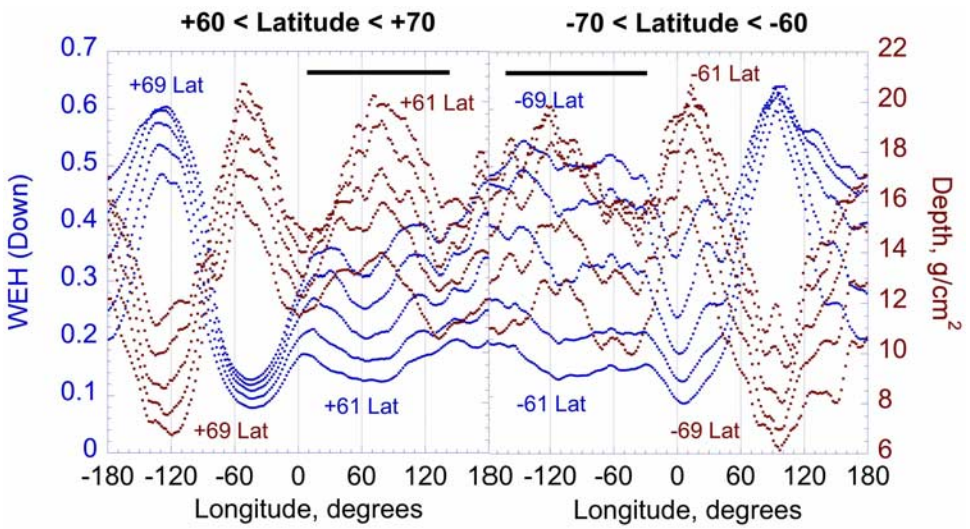

Figure 2. Longitude scans of the water mass fractions of the lower layer (in blue) and the apparent burial depths (in red) for five latitudes between 60° and 70°.

between −75° and −65°, and between +65° and +75° Latitude. Data between 61° and 63° were not included here because, as will be seen later, contributions to WEH abundances from hydrated minerals became more noticeable equatorward of 65°. Regressions between Wdn determined from assumptions of 5 wt. % rather than 1 wt. % yielded a systematic reduction in Wdn by about 5% [*Bandfield and Feldman*, 2008]. A similar regression showed that the burial depth was increased by about 33% when the WEH of the upper layer was increased from 1 wt. % to 5 wt. %. Note that these two estimates are unidirectional because the WEH content of the upper layer is not expected to be less than 1 wt. % [*Feldman et al.*, 2004].

[9] In order to estimate the systematic error expected to result from our uncertainty in choice of composition other than hydrogen, we determined the sensitivity of Wdn and D to compositions characterized by macroscopic absorption cross sections at the plus and minus half widths at half maxima of the histogram derived by *Diez et al.* [2008] from the compositions measured by both Mars Exploration Rovers (MER) (the *Diez et al.* [2008] compositions 20 and 22) [*Rieder et al.*, 2004; *Gellert et al.*, 2006]. Regressions for Wdn derived from these two compositions yielded an uncertainty amounting to±3% from that derived using the mean composition (composition 21 of *Diez et al.* [2008]) and for D, the uncertainty amounted to±10% from the mean. These two estimates of uncertainties cannot be combined with those derived from our uncertainty in the water content of the upper layer because those derived from composition are bidirectional, not unidirectional.

3. Distributions of Wdn and D and Their Intercorrelations

[10] Maps of Wdn and D are shown in stereographic projection poleward of ±45° in Figure 1 [see also *Diez et al.*, 2008; *Feldman et al.*, 2007]. The data poleward of 75°S were not included in these maps because of contamination of the measured thermal neutron currents coming from the very large flux of thermal neutrons that leak from the CO_2-covered, residual south polar cap. Several points are worth special notice. First, the maximum Wdn abundance is centered on the north residual polar cap, as is expected because this water-ice deposit is known from IR observations [e.g., *Kieffer et al.*, 1976] to be fully exposed to the atmosphere. Second, each hemisphere shows a well-defined secondary maximum between about 65° and 75° latitude. These maxima are nearly equal at between 55% and 65% WEH mass percent. Third, there is a ring of enhanced apparent burial depths in both hemispheres centered at about 60° latitude. These relative maxima reflect the equatorward margin of stable water ice at high latitudes predicted by theories of the diffusion of water vapor from the atmosphere to the subsurface [*Leighton and Murray*, 1966; *Farmer and Doms*, 1979; *Fanale et al.*, 1986; *Mellon and Jakosky*, 1993; *Schorghofer and Aharonson*, 2005], and also the boundary between where water molecules have a dominant molecular association with hydrated minerals equatorward of these rings, and where they reside mostly as water ice poleward of these rings (see, e.g., discussion of *Feldman et al.* [2007] and references therein). Both rings show relative minimum depths at those longitudes where the Wdn abundances are maximum. And lastly, poleward of both rings, the apparent burial depths decrease monotonically with increasing latitude, also in agreement with predictions [*Leighton and Murray*, 1966; *Farmer and Doms*, 1979; *Fanale et al.*, 1986; *Mellon and Jakosky*, 1993; *Schorghofer and Aharonson*, 2005].

[11] A comparison between longitude scans of the WEH of the lower layer, Wdn, and their burial depths are shown in Figure 2 for five latitudes between 60° and 70° north and south latitudes. A close inspection shows that Wdn in both hemispheres increases monotonically with increasing latitude at any given longitude within this latitude range, and the apparent burial depths decrease monotonically with increasing latitude. We note especially that in each hemisphere and latitude zone, the longitudinal dependence of Wdn displays a coherent relative maximum, a relative minimum, and a range of longitudes where Wdn is roughly

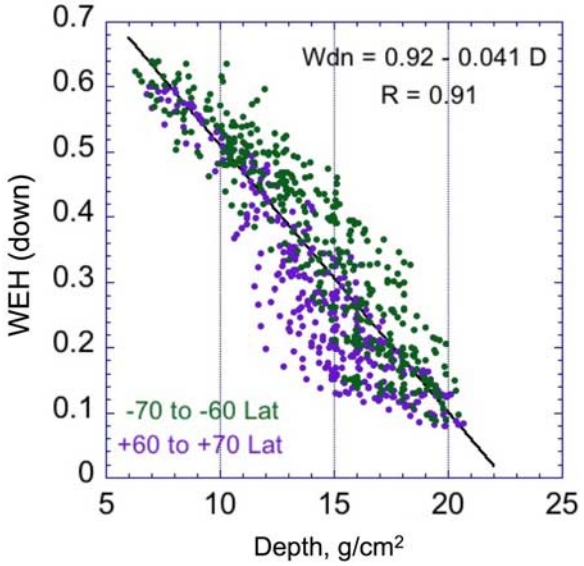

Figure 3. Correlation between the water mass fraction of the lower layers and their apparent burial depths. The south is plotted using green symbols, and the north uses lavender.

constant. The thick black lines in both north and south latitude zones delineate these last ranges of longitudes.

[12] It is also evident from Figure 2 that Wdn is generally anticorrelated with burial depth. We emphasize that this anticorrelation is evident in each of the constant latitude cuts of Wdn and D as well as in each of the constant longitude cuts of Wdn and D. The overall anticorrelation is shown explicitly in Figure 3. The regression that best fits the summed data set in both hemispheres is given by

$$\mathrm{Wdn} = 0.92 - 0.041\mathrm{D}. \quad (1)$$

The correlation coefficient for this regression is high (R = 0.91). A close inspection of Figure 3 shows that the Wdn abundances in the south (green dots) are generally larger than those in the north (lavender dots). We note that the regression predicts a WEH mass fraction at zero depth of 0.92, which, perhaps coincidentally, is close to the water-ice content of both the northern and southern polar layered deposits inferred from the MARSIS radar experiment [*Plaut et al.*, 2007].

[13] We will now concentrate on the northern and southern longitudinal zones for which Wdn is most nearly constant at each latitude. These two zones are positioned adjacent to each other in Figure 2. An overlay of the latitudinal dependences of zonal averages of Wdn in each hemisphere is shown in Figure 4. The vertical error bars give the standard deviation of Wdn within each zone at each latitude. We note that the abundance of Wdn in the south is clearly larger by about 16 weight percent than that in the north for latitudes poleward of 63°.

[14] The data equatorward of 61° in Figure 4 needs to be discounted because significant contributions to Wdn from hydrated minerals become very noticeable [*Feldman et al.*, 2007], as seen by the relative maximum in D in Figure 1. Intercomparison between northern and southern Wdn therefore no longer corresponds only to soil water-ice content.

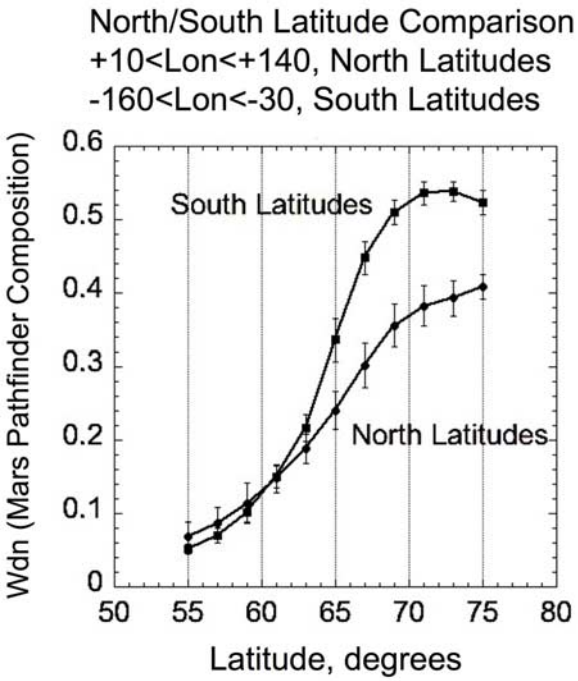

Figure 4. An overlay of the latitudinal dependences of zonal averages of Wdn in each hemisphere. The error bars give the standard deviation of all values going into the averages at each latitude.

Their ratio (shown in Figure 5) reaches a broad maximum between 65° and 73° latitude. The apparent decrease in this ratio at 75° needs to be discounted, however, for two separate reasons. First, the broad spatial response function of MONS is beginning to pick up the signal from the

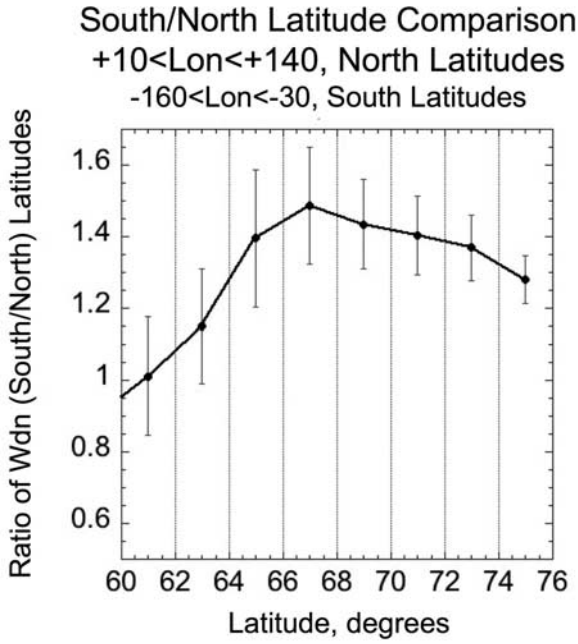

Figure 5. Ratio of zonal averages of Wdn in the south to those in the north as a function of latitude between 60° and 75°.

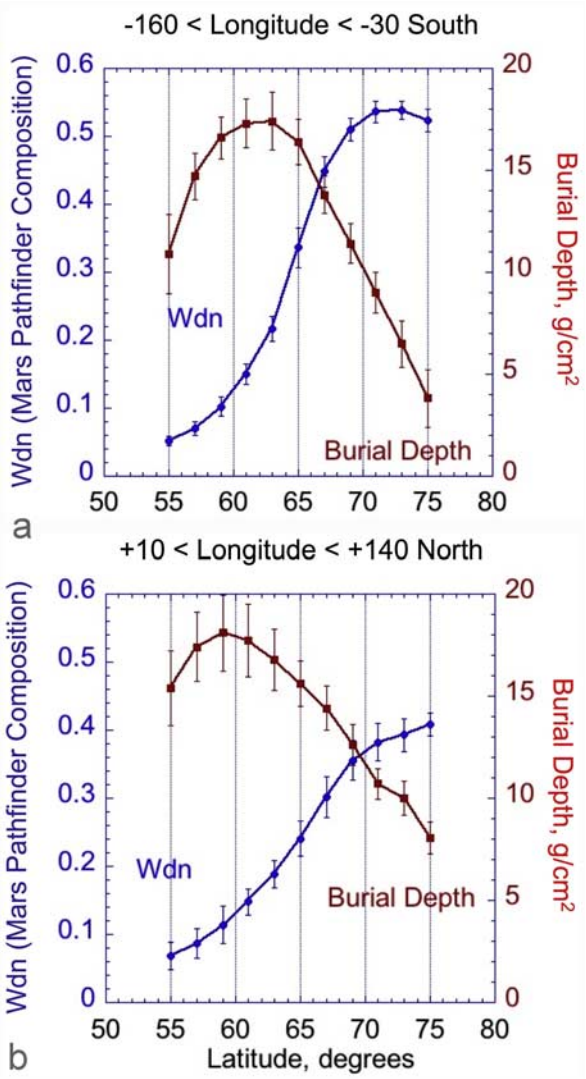

Figure 6. (a) Comparison between the lower layer water mass fractions (blue) and apparent burial depths (red) averaged over the longitude ranges identified by the thick horizontal bars shown in Figure 2 at high northern latitudes. (b) Comparison between the lower layer water mass fractions (blue) and apparent burial depths (red) averaged over the longitude ranges identified by the thick horizontal bars shown in Figure 2 at high southern latitudes.

outlying ring of surficial water ice that surrounds Olympia Undae in the north [*Tanaka and Scott*, 1987], and second, the CO_2 veneer that covers the south-residual cap [*Kieffer*, 1979] contaminates the measurement of thermal neutron currents poleward of about 75° S. The broad maximum in Figure 5 between 65° and 75° amounts to a factor of 1.4 ± 0.1 between Wdn in the southern and northern high latitudes. Alternately, it corresponds to a difference of (54−38) = 16 weight percent of WEH as seen in Figure 4.

[15] A comparison between the apparent burial depths averaged over these longitudinal zones as a function of latitude is shown in Figure 6. Although each zone displays the same general trend with latitude, that in the south is steeper than that in the north poleward of 65°. A closer inspection shows that this effect is just what is expected from the general anticorrelation between Wdn and D shown in Figure 3. The burial depths at high northern latitudes are larger than those in the south in concert with the fact that the Wdn abundances are larger in the south than in the north.

4. Summary

[16] Distributions of WEH within assumed semi-infinite, buried permafrost layers are intercompared within latitude zones between 60° and 75° in the northern and southern hemispheres of Mars. The purpose of this intercomparison is to quantify any potential asymmetries that could provide important clues regarding the thermophysical and/or mineralogic compositional structure of surface soils, and perhaps, the emplacement mechanism and relative timing of the WEH deposition. We found that indeed, these asymmetries are present, although the overall Wdn contents below a desiccated surface layer and their burial depths, are similar. Overall, the WEH abundance in the south is larger than that in the north. Their ratio in longitude zones in which they are nearly constant in each hemisphere maximizes at a factor of 1.4 ± 0.1, or equivalently 16 weight percent WEH abundance between 64° and 74° latitude. Regardless of this asymmetry, WEH deposits in both hemispheres are anticorrelated with burial depth through nearly the same regression relation, given by equation (1). Additionally, the burial depths are observed to decrease monotonically with increasing latitude in both hemispheres within this latitudinal range. We now explore possible implications of all of these findings for the pore-fraction structure of surface soils, the potential depth dependence of mineralogy, and potentially time-dependent delivery mechanisms for near-surface water molecules.

5. Discussion

[17] We discuss first the strong anticorrelation between Wdn and D shown in Figure 3. It should bear strongly on the depth dependence of open pore volume in, or water-ice holding capacity of, near-surface regolith. However, its interpretation is not unique because it also depends on the source and emplacement mechanism of subsurface water molecules, the relationships between burial depth, groundcover thermal inertia, albedo, latitude, and the partition of water molecules between water ice and water of hydration. In this last regard, we note again that neutrons cannot separate water of hydration from water ice. However, if the dominant molecular association of hydrogen is in the form of water ice at high latitudes, then a likely delivery mechanism is the diffusion of water molecules into surface soils from the atmosphere and/or the precipitation of water ice onto the surface followed by their diffusion into surface soils. This process is then followed by their freeze-out to water ice on contact with the cold soil grains that surround open pore volumes.

[18] These water vapor molecules can also hydrate minerals within the soil in competition with the formation of water ice. We note though that most current models of this process [*Mellon et al.*, 2004; *Schorghofer and Aharonson*, 2005] can predict only the equilibrium burial depth, D, of the resultant permafrost layer, not the water content, Wdn,

of this layer. Intercomparison between burial depths inferred from MONS neutron data and the model predictions at high latitudes show generally quantitatively good agreement [*Diez et al.*, 2008]. Comparison of the burial depths determined using the MONS data with depths determined using seasonal variations in temperatures measured using the Thermal Emission Spectrometer (TES) data [*Bandfield and Feldman*, 2008] also shows generally good quantitative agreement.

[19] Although there have been no previous predictions of the very strong anticorrelation between Wdn and D shown in Figure 3, its simplest interpretation is that on average, the open pore volumes of near-surface regolith must decrease with increasing depth. However, this interpretation needs to be qualified for several reasons. First and foremost is that the 2-D model we are using to interpret neutron counting-rate data from Mars orbit may not apply to realistic surface-regolith structure. Multiple layers having lateral structure smaller than the MONS field of view may be more realistic. Next, the depth of view for the information content of neutrons that leak upward from planetary surfaces depends strongly on the water content of the regolith. This depth is controlled by the mean scattering lengths for elastic scattering and energy loss in the epithermal range of energies, between about 0.1 eV and 500 keV. If the regolith contains no water, then typical elastic-scattering lengths are about 10 g/cm^2 and typical mean energy-loss lengths are just above 100 g/cm^2 [*Feldman et al.*, 1993]. However, addition of water reduces the energy-loss scattering length considerably, given by

$$\Lambda_{el} = 0.744\ \mathrm{WEH}^{-0.977}\ \mathrm{g/cm^2}, \tag{2}$$

where WEH is restricted to the mass-fraction range between 0.1 and 1.0, and Λ_{el} is the mean energy-loss scattering length. Equation (2) gives $0.74 < \Lambda_{el} < 7.0$ g/cm^2 for $0.1 <$ WEH < 1.0. This scattering-length range therefore reduces the neutron depth of view to less than about 10 cm from the top of the permafrost layer if we choose a density of about 1.5 g/cm^3. In other words, neutron spectroscopy from orbit provides water-content information only about the upper ~10 cm of the permafrost layer in areal patches of surface material having spot-size dimensions of about 600 km for latitudes between about 60° and 75° on Mars.

[20] Of course, other explanations are also possible. Latitude by itself cannot be the cause of the anticorrelation effect shown in Figure 3 because a detailed inspection of Figure 2 shows that this anticorrelation occurs both as a function of latitude for a given longitude, as well as a function of longitude for a given latitude. Of the remaining three factors, TES data shows that surface-cover thermal inertia dominates over latitude or albedo [*Bandfield and Feldman*, 2008]. Unfortunately, we do not have enough information from orbital data to determine the depth dependence of thermal inertia of the surface cover in the absence of water ice because interpretation of observed surface temperatures from orbit suffers from similar (but different) ambiguities to those mentioned above for neutrons [*Bandfield and Feldman*, 2008].

[21] Other uncertainties are that the open pore volumes may not fill completely, uniformly with depth [*Bandfield and Feldman*, 2008]. For example, the regression shown in Figure 3 may reflect a reduced filling of open pore volumes with increasing depth that occurred during some past climate era. The burial depth at the present time then reflects the present-day temperature and relative humidity at the surface averaged over a time period of less than ~10,000 years [*Montmessin et al.*, 2007; *Feldman et al.*, 2008]. In addition, the assumption of pure water ice with no contribution from hydrated minerals, may not be correct. Indeed, if the fractional contribution from hydrated minerals is modest to small at high latitudes, then large pore volumes are required when Wdn gets large. Choosing a fractional contribution from hydrated minerals to be zero, a soil-grain density of 2.65 g/cm^3, and an ice density of 0.92 g/cm^3, these volumes must be 24.3%, 41.9%, 55.3%, 65.8%, 74.2%, and 81.2% for water-ice mass percentages of 10%, 20%, 30%, 40%, 50%, and 60%, respectively. However, if there is a sufficiently thick near-surface soil layer containing, say, 10% by weight of anhydrous $MgSO_4$, then the 11-hydrate of $MgSO_4$ would be stable [*Vaniman et al.*, 2007] leading to an additional 16.5 wt. % WEH.

[22] Another possible delivery mechanism is that the water ice falls to the surface in the form of snow or hail [see, e.g., *Mischna et al.*, 2003; *Levrard et al.*, 2004, 2007; *Montmessin et al.*, 2004; *Montmessin*, 2006, and references therein]. In this case, the initial water-ice mass fraction at the surface can be quite large if deposition happens more quickly during some parts of the year than sublimation happens at other parts, leading to a net growth of surface water-ice cover. Indeed, this process can lead to a large Wdn content of surface regolith over a short time [*Levrard et al.*, 2004; *Montmessin*, 2006; *Montmessin et al.*, 2007]. A study of the diameters of bare and water-ice-coated dust particles at the Viking 2 landing site yielded average bare dust diameters of about 1 micron and diameters of composite water-ice and dust particles of between 2 and 3 microns [*Pollack et al.*, 1977]. If we assume spherical dust and ice-covered dust respectively, the mass fraction of water ice in the composite ice particles is

$$M_i = \left\{1 + (\rho_d/\rho_i)/\left[(r_o/r_d)^3 - 1\right]\right\}^{-1}. \tag{3}$$

Here, M_i is the mass fraction of water ice, ρ_d is the density of the dust core, 2.65 g/cm^3, ρ_i is the density of the ice rind, 0.92 g/cm^3, r_o is the radius of the outside of the total ice-covered dust particle, and r_d is the radius of the inner dust particle. Choosing $(r_o/r_d) = 2$ and 3 in accordance with those found by *Pollack et al.* [1977], we get $M_i = 0.71$ and 0.90, respectively. Because the only true unknown parameter in equation (3) is r_o/r_d, these estimates for M_i could be generally valid and we could then account for the observations shown in Figures 2 and 3 if, during times when the high-latitude terrains poleward of ±55° are covered by the polar hood in the fall and winter seasons in both hemispheres [*Montmessin et al.*, 2004; *Levrard et al.*, 2004], water ice in the form of hail or snow falls to the ground. This process will be aided by regional dust storms that occur at the margins of both the advancing and retreating seasonal CO_2 ice deposits [*Cantor*, 2007], thereby providing enhanced nucleation centers for hail formation and lag deposits that cover the hail or snow after it covers the ground. Regardless of whether precipitation can account for the observed WEH content of

high-latitude terrain, it is far from certain that it will produce the depth-dependent structure of water-ice content shown in Figure 3.

[23] Another possibility is that the presently observed WEH content of high-latitude soils is a remnant of water-ice migration driven by the return to lower obliquities from the general high-obliquity state of Mars that occurred about 4 million years (Ma) ago [*Levrard et al.*, 2004, 2007] or from more recent precession states of the Martian spin axis at perihelion [*Montmessin et al.*, 2007]. If obliquity variations provide the explanation, then very little desiccation must have occurred during the past ~1 Ma in the top few tens of cm between 60° and 75°. However, the generally large obliquity variations and attendant large variations in solar heat input to high-latitude surface soils in the past 1 Ma [*Levrard et al.*, 2007] seems to make this possibility unlikely. In addition, any potential surface deposition during past climate cycles would then sublimate away on a timescale that is less than about 10,000 years [*Montmessin et al.*, 2007; *Feldman et al.*, 2008] to produce Wdn distributions that are in equilibrium with the present climate, which favors the northern lowlands [*Montmessin et al.*, 2007], not the southern highlands, as observed. These explanations also suffer from the difficulty in explaining the observed generally larger ice-filled pore volumes at lower depths beneath the surface.

[24] In order to be accepted, this entire mechanism, which starts with the atmospheric global circulation, the self-consistent dust generation in regional dust storms, the formation of water-ice covered dust-nucleation centers, and the advection of water-ice particles while picking up an additional CO_2 ice coating to reduce its float time, and ending with their precipitation to the surface, needs to be carefully simulated (see the pictorial description of this process given by *Montmessin et al.* [2004]). Furthermore, these simulations need to follow the seasonal recession of the CO_2 cap in the spring and summer in each hemisphere, leading to the diffusion of water vapor into open regolith pore spaces, and their subsequent freeze-out beneath the surface [*Schorghofer and Aharonson*, 2005]. The air-fall dust generated during regional dust storms [*Cantor*, 2007] could then add to this process by percolating through, and providing a lag cover for, the ice-covered dust particles that sit on the ground. The sequence of these events must then be able to leave more open pore volume near the surface than at depth. In addition, the observed lag cover of thickness D (ranging between about 4.5 cm and 13.5 cm given in Figure 3) must be sufficient to protect the lower water-ice rich layer from sublimation during the past, approximately 4 Ma.

[25] Another potential explanation for Figure 3 is in terms of water ice trapped within thermal cracks in polygonally fractured terrain [see, e.g., *Mellon*, 1997; *Mangold*, 2005; *Mellon et al.*, 2007]. This explanation is supported by the fact that polygonal terrain observed at high latitudes on Mars does indeed preferentially populate the latitude zones between 60° and 75° [*Mangold et al.*, 2004; *Mangold*, 2005; *Mellon et al.*, 2007]. In addition, the analysis of surface frost observations at the Viking Lander 2 site gives this end-to-end scenario plausibility by restricting the dispersal of newly sublimated water-vapor molecules in the spring by their re-adsorption onto nearby surfaces because the rise in atmospheric temperatures lags the rise in surface temperatures when the sun rises above the horizon in the spring, thereby delaying desiccation of near-surface regolith by about 35 sols [*Svitek and Murray*, 1990]. This extra time will promote the downward pumping of atmospheric water molecules driven by the seasonal thermal wave that was modeled by *Schorghofer and Aharonson* [2005].

[26] Other possibilities may also account for the observations shown in Figures 2 and 3. However, none (including the aforementioned ones) have been pursued quantitatively. For example, differing burial depths of hydratable salt evaporates caused by differences in the layering of brine aquifers, or differences in their precipitation and attendant runoff patterns when Mars was warmer and wetter during the late Noachian and early Hesperian periods, could help explain why the southern highlands contain more WEH than the northern Vastitas Borealis Formation lowlands. An explanation to the observed asymmetry between WEH distributions at high Martian latitudes must therefore await theoretical attention and/or more, and different experimental information, such as is promised from the upcoming landing of the Phoenix spacecraft near 70° N latitude of Mars [*Smith and Phoenix Science Team*, 2007]. Nevertheless, our present results, which reveal a strong general anticorrelation between burial depth and WEH content of a lower layer, Wdn, between 60° and 75° latitude, and Wdn deposits that are larger in the south than in the north pose an important interpretational challenge.

[27] **Acknowledgments.** We wish to thank N. Mangold, F. Costard, F. Forget, and A. Pathari for many useful discussions regarding the interpretations of our data. This work was supported in part by the NASA Mars Odyssey program and was carried out under the auspices of the Planetary Science Institute.

References

Bandfield, J. L., and W. C. Feldman (2008), Martian high-latitude permafrost depth and surface cover thermal inertia distributions, *J. Geophys. Res.*, doi:10.1029/2007JE003007, in press.

Cantor, B. A. (2007), Present-day Martian weather: 5 Mars years of observations by MGS-MOC and MRO-MARCI, paper presented at Seventh International Conference on Mars, Lunar and Planet. Inst., Pasadena, Calif., 9–13 July.

Diez, B., W. C. Feldman, S. Maurice, O. Gasnault, T. H. Prettyman, M. T. Mellon, O. Aharonson, and N. Schorghofer (2008), H layering in the top meter of Mars, *Icarus*, in press.

Fanale, F. P., J. R. Salvail, A. P. Zent, and S. E. Postawko (1986), Global distribution and migration of subsurface ice on Mars, *Icarus*, *67*, 1–18, doi:10.1016/0019-1035(86)90170-3.

Farmer, C. B., and P. E. Doms (1979), Global seasonal variation of water vapor on Mars and the implications of permafrost, *J. Geophys. Res.*, *84*, 2881–2888.

Feldman, W. C., W. V. Boynton, B. M. Jakosky, and M. T. Mellon (1993), Redistribution of subsurface neutrons caused by ground ice on Mars, *J. Geophys. Res.*, *98*, 20,855–20,870.

Feldman, W. C., et al. (2004), The global distribution of near-surface hydrogen on Mars, *J. Geophys. Res.*, *109*, E09006, doi:10.1029/2003JE002160.

Feldman, W. C., M. T. Mellon, O. Gasnault, B. Diez, R. C. Elphic, J. J. Hagerty, D. J. Lawrence, S. Maurice, and T. H. Prettyman (2007), Vertical distribution of hydrogen at high northern latitudes on Mars: The Mars Odyssey Neutron Spectrometer, *Geophys. Res. Lett.*, *34*, L05201, doi:10.1029/2006GL028936.

Feldman, W. C., M. T. Mellon, O. Gasnault, S. Maurice, and T. H. Prettyman (2008), Volatiles on Mars: Scientific results from the Mars Orbital Neutron Spectrometer, in *The Martian Surface: Composition, Mineralogy, and Physical Properties*, edited by J. F. Bell III, Cambridge Univ. Press, New York.

Gellert, R., et al. (2006), Alpha Particle X-Ray Spectrometer (APXS): Results from Gusev crater and calibration report, *J. Geophys. Res.*, *111*, E02S05, doi:10.1029/2005JE002555.

Kieffer, H. H. (1979), Mars south polar spring and summer temperatures: A residual CO_2 frost, *J. Geophys. Res.*, *84*, 8263–8288.

Kieffer, H. H., T. Z. Martin, S. C. Chase, E. D. Miner, and F. D. Palluconi (1976), Martian north pole summer temperatures: Dirty water ice, *Science*, *194*, 1341–1344, doi:10.1126/science.194.4271.1341.

Leighton, R. B., and B. C. Murray (1966), Behavior of carbon dioxide and other volatiles on Mars, *Science*, *153*, 136–144, doi:10.1126/science.153.3732.136.

Levrard, B., F. Forget, F. Montmessin, and J. Laskar (2004), Recent ice-rich deposits formed at high latitudes on Mars by sublimation of unstable equatorial ice during low obliquity, *Nature*, *431*, 1072–1075, doi:10.1038/nature03055.

Levrard, B., F. Forget, F. Montmessin, and J. Laskar (2007), Recent formation and evolution of northern Martian polar layered deposits as inferred from a Global Climate Model, *J. Geophys. Res.*, *112*, E06012, doi:10.1029/2006JE002772.

Mangold, N. (2005), High latitude patterned grounds on Mars: Classification, distribution and climatic control, *Icarus*, *174*, 336–359, doi:10.1016/j.icarus.2004.07.030.

Mangold, N., S. Maurice, W. C. Feldman, F. Costard, and F. Forget (2004), Spatial relationships between patterned ground and ground ice detected by the Neutron Spectrometer on Mars, *J. Geophys. Res.*, *109*, E08001, doi:10.1029/2004JE002235.

Maurice, S., W. C. Feldman, T. H. Prettyman, B. Diez, and O. Gasnault (2007), Reduction of Mars Odyssey Data, *Lunar Planet. Sci.*, *XXXVIII*, abstract 2036.

Mellon, M. T. (1997), Small-scale polygonal features on Mars: Seasonal thermal contraction cracks in permafrost, *J. Geophys. Res.*, *102*, 25,617–25,628.

Mellon, M. T., and B. M. Jakosky (1993), Geographic variations in the thermal and diffusive stability of ground ice on Mars, *J. Geophys. Res.*, *98*, 3345–3364.

Mellon, M. T., W. C. Feldman, and T. H. Prettyman (2004), The presence and stability of ground ice in the southern hemisphere of Mars, *Icarus*, *169*, 324–340, doi:10.1016/j.icarus.2003.10.022.

Mellon, M. T., M. L. Searls, S. Martinez-Alonso, and the HIRISE Team (2007), HIRISE observations of patterned ground on Mars, paper presented at Seventh International Conference on Mars, Lunar and Planet. Inst., Pasadena, Calif., 9–13 July.

Mischna, M. A., M. I. Richardson, R. J. Wilson, and D. J. McCleese (2003), On the orbital forcing of Martian water and CO_2 cycles: A general circulation model study with simplified volatile schemes, *J. Geophys. Res.*, *108*(E6), 5062, doi:10.1029/2003JE002051.

Montmessin, F. (2006), The orbital forcing of climate changes on Mars, *Space Sci. Rev.*, *125*, 457–472, doi:10.1007/s11214-006-9078-x.

Montmessin, F., F. Forget, P. Rannour, M. Cabane, and R. M. Haberle (2004), Origin and role of water ice clouds in the Martian water cycle as inferred from a general circulation model, *J. Geophys. Res.*, *109*, E10004, doi:10.1029/2004JE002284.

Montmessin, F., R. M. Haberle, F. Forget, Y. Langevin, R. T. Clancey, and J. -P. Bibring (2007), On the origin of perennial water ice at the south pole of Mars: A precession controlled mechanism, *J. Geophys. Res.*, *112*, E08S17, doi:10.1029/2007JE002902.

Plaut, J. J., et al. (2007), Subsurface radar sounding of the south polar layered deposits of Mars, *Science*, *316*, 92–95, doi:10.1126/science.1139672.

Pollack, J. B., D. Colburn, R. Kahn, J. Hunter, W. Van Camp, C. E. Carlston, and M. R. Wolf (1977), Properties of aerosols in the Martian atmosphere, as inferred from Viking Lander imaging data, *J. Geophys. Res.*, *82*, 4479–4496.

Prettyman, T. H., et al. (2004), Composition and structure of the Martian surface at high southern latitudes from neutron spectroscopy, *J. Geophys. Res.*, *109*, E05001, doi:10.1029/2003JE002139.

Rieder, R., et al. (2004), Chemistry of rocks and soils at Meridiani Planum from the Alpha Particle X-Ray spectrometer, *Science*, *306*, 1746–1749, doi:10.1126/science.1104358.

Schorghofer, N., and O. Aharonson (2005), Stability and exchange of subsurface ice on Mars, *J. Geophys. Res.*, *110*, E05003, doi:10.1029/2004JE002350.

Smith, D. E., et al. (1999), The global topography of Mars and implications for surface evolution, *Science*, *284*, 1495–1507, doi:10.1126/science.284.5419.1495.

Smith, M. D. (2002), The annual cycle of water vapor on Mars as observed by the Thermal Emission Spectrometer, *J. Geophys. Res.*, *107*(E11), 5115, doi:10.1029/2001JE001522.

Smith, P. H., and Phoenix Science Team (2007), The Phoenix Mission, paper presented at Seventh International Conference on Mars, Lunar and Planet. Inst., Pasadena, Calif., 9–13 July.

Svitek, T., and B. Murray (1990), Winter Frost at Viking Lander 2 site, *J. Geophys. Res.*, *95*, 1495–1510.

Tanaka, K. L., and D. H. Scott (1987), Geologic map of the polar regions of Mars, *U.S. Geol. Surv. Misc. Geol. Invest. Map*, *1-1802-C*.

Vaniman, D. T., S. J. Chipera, D. L. Bish, and R. C. Peterson (2007), Mars latitude, Mars obliquity, and hydration states of Mg-sulfates, paper presented at Seventh International Conference on Mars, Lunar and Planet. Inst., Pasadena, Calif., 9–13 July.

Wänke, H., J. Brückner, G. Dreibus, R. Rieder, and I. Ryabchikov (2001), Chemical composition of rocks and soils at the Pathfinder site, *Space Sci. Rev.*, *96*, 317–330, doi:10.1023/A:1011961725645.

J. L. Bandfield, Department of Earth and Space Sciences, University of Washington, Seattle, WA 98115-1310, USA.

B. Diez and S. Maurice, Centre d'Etude Spatiale des Rayonnements, F-31028 Toulouse, France.

R. C. Elphic, NASA Ames Research Center, Moffett Field, CA 94035-1000, USA.

W. C. Feldman, Planetary Science Institute, 1700 East Fort Lowell, Suite 106, Tucson, AZ 85719-2395, USA. (feldman@psi.edu)

S. M. Nelli, Atmospheric, Oceanic and Space Sciences, University of Michigan, Ann Arbor, MI 48109, USA.